Supporting Information

A Metal-Organic Framework of Organic Vertices and Polyoxometalate Linkers as a Solid-State Electrolyte

Wentao Xu,[†] Xiaokun Pei,[†] Christian S. Diercks,[†] Hao Lyu,[†] Zhe Ji,[†] and Omar M. Yaghi*[,†,‡]

[†]Department of Chemistry, University of California-Berkeley; Materials Sciences Division, Lawrence Berkeley National Laboratory; and Kavli Energy NanoSciences Institute, Berkeley, California 94720, United States

[‡]UC Berkeley-KACST Joint Center of Excellence for Nanomaterials for Clean Energy Applications, King Abdulaziz City for Science and Technology, Riyadh 11442, Saudi Arabia

Table of Contents

Section S1 General Methods and Materials

Chemicals. All starting materials and solvents, unless otherwise specified, were obtained from Sigma-Aldrich Chemicals, and used without further purification. Bis(trifluoromethanesulfonyl)imide (LiTFSI) (purity ≥ 98 %) was purchased from TCI. Lithium metal chips, $LiFePO_4$, Super C45 conductive carbon, Polyvinylidene fluoride (pvdf) and CR2032 coin cells were purchased from MTI. $[N(C_4H_9)_4]_3[MnMo_6O_{18}\{(OCH_2)_3CNH_2\}_2]$ ($MnMo_6$) and tetrakis(4-formylphenyl)methane (TFPM) were synthesized according to literature reports.[1,2]

Analytical techniques and instruments. Attenuated total reflectance Fourier-transform infrared spectroscopy (FT-IR) of solid samples was performed on a Bruker ALPHA Platinum ATR-FT-IR spectrometer equipped with a single reflection diamond ATR module. All spectra were collected neat in ambient atmosphere. The signals are given in transmittance (%) against wavenumbers (cm^{-1}).

^1H NMR spectra were acquired on a Bruker AVQ-400 NMR spectrometer.

Scanning electron microscopy (SEM) images were recorded on a FEI Quanta 3D FEG scanning electron microscope with an accelerating voltage of 10 kV and a working distance of 10.0 mm.

Thermogravimetric analysis (TGA) curves were recorded on a TA Q500 thermal analysis system under nitrogen flow, ramping at 5 °C min^{-1} from room temperature to 800 ˚C. Ultrahigh-purity-grade N_2 was used in all TGA measurements

Inductively Coupled Plasma-Optical Emission Spectrometry (ICP-OES) experiments were carried out on a Perkin Elmer Optima 7000 spectrometer. The samples were digested in a solution of 67–70% nitric acid (1.0 mL) and 48% hydrofluoric acid (0.1 mL) for 15 min and diluted with Milli-Q water to 35.00 mL before the measurement.

Powder X-ray diffraction (PXRD) patterns were recorded using a Rigaku Miniflex 600 diffractometer (Bragg-Brentano geometry, Cu Kα radiation $\lambda = 1.54056$ Å).

Electrochemical measurements were carried out using a Bio-logic VMP3 potentiostat/galvanostat.

Single-crystal X-ray diffraction (SXRD) data was collected using synchrotron radiation at beamline 12.2.1 of the Advanced Light Source, Lawrence Berkeley National Laboratory (LBNL). Beamline 12.2.1 is equipped with a PHOTON-II CMOS detector operating in shutterless mode, and the radiation is monochromated using silicon (111).

Section S2. Synthetic Procedures

MOF-688: 1000 mg of $[N(C_4H_9)_4]_3[MnMo_6O_{18}\{(OCH_2)_3CNH_2\}_2]$ ($MnMo_6$) and 110 mg of tetrakis(4-formylphenyl)methane (TFPM) were dissolved in a mixture of 10 mL anhydrous acetonitrile and 10 mL of anhydrous dioxane. Then 500 mL of acetic acid were added, and the solution was transferred into four 20 mL vials. The vials were placed in an oven at 100 °C for 2 days. The resulting solid was collected *via* filtration. Solvent exchange was performed with anhydrous *N*,*N*-dimethylformamide at room temperature (40 mL × 3) over 24 hours, and with anhydrous acetonitrile at room temperature (40 mL × 6) over 2 days. The obtained solid was collected *via* filtration and dried under vacuum to yield MOF-688 (650 mg, 61% based on TFPM). Elemental Analysis: for C141H260Mn2Mo2N10O48: Calcd. C 41.06%, H 6.35%, N 3.40%, Mn 2.66%, Mo 27.91%, Found C 40.06%, H 6.32%, N 3.20%, Mn 2.64%, Mo 26.61%.

Ion exchange on MOF-688: 200 mg of MOF-688 was immersed in 5 mL of 1 M acetonitrile solution of LiTFSI at room temperature. The solution was changed three times per day over two days. The process was monitored by digestion ^{1}H NMR, where peaks assigned to TBA^+ disappeared upon cation exchange. Then the ion exchanged MOF-688 was immersed in fresh anhydrous acetonitrile (40 mL × 6) over two days to remove excess lithium salt in the pores. TBA^+ was reintroduced into MOF-688 by immersing MOF-688 in 1 M acetonitrile solution of TBABr (10 mL × 3) for one day.

Section S3 Single-Crystal X-ray Analysis of MOF-688

A single crystal of POM-COF was mounted on MiTeGen® kapton loops in LV CryoOil® and placed in a 100(2) K nitrogen cold stream from an Oxford Cryosystems Cryostream equipment. The data was collected to $\sin(\theta)/\lambda = 0.625$ with combined phi and omega scans. The raw data were processed with the Bruker APEX3 V8.38 software.[1] The data were first integrated using the SAINT and then corrected for absorption with SADABS.[1,2] Based on intensity statistics table for the whole dataset (PRP file), the resolution was cut off to 0.95 Å ($R_{merge} \leq 40\%$ or average $I/\sigma > 2.5$ for the highest resolution shell). The structures were solved by dual space (SHELXT-2014/05) and the refinement was done by full-matrix least squares on F^2 (SHELXL-2018),[3,4] using the Olex^2 software package.[5]

Space group determination process always suggest $I4_1/amd$ as the most possible space group. However, when trying to lower space group symmetry, it is found that R_{int} at resolution = 0.95 Å in $I4_1/a$ is 7.25%, while R_{int} at resolution = 1.00 Å in $I4_1/amd$ is 8.28%, which indicates that $I4_1/amd$ is higher pseudo-symmetry. Also, refinement on the structure in $I4_1/amd$ also indicates that $I4_1/amd$ is a space group with higher pseudo-symmetry: in the $I4_1/amd$ structure, TFPM units sit on inversion centers where two perpendicular mirror planes also pass through. The mirror planes fixed the benzene rings to be in the planes, showing a conformation which is chemically incorrect. Therefore, the space group is assigned to $I4_1/a$.

The TFPM unit in the structure shows a significant rotational disorder of the benzene rings. Therefore, the benzene ring is split into to two positions during the refinement (C6A ~ C10A, C6B ~ C10B). The occupancy of each split position was constrained to 0.5. SADI, FLAT, ISOR, EADP were applied to restrain the unstable anisotropic refinement on the benzene rings. The disorder in the TFPM unit also affects the conformation of the imine bonds, so the imine bonds were also split into two positions (C5A-N1A, C5B-N1B). The positional disorder of imine bonds further propagates to the $MnMo_6$ unit, as reflected in the relatively large ellipsoids of it. These ellipsoids were not split because the ellipsoid shapes are relatively spherical, indicating it is the overlap of several disordered states over all directions.

During the refinement, the electron densities of two symmetrically equivalent tetrabutylammonium (TBA) cations per POM unit can be observed in the pore. Stoichiometrically, there is one more TBA^+ per POM unit in the pore to balance the charge of $MnMo_6$, however, it is likely to be too disordered to be observed crystallographically. Refinement trails to assign the clearer TBA cation indicate that it is actually quite disordered, as observed from large Uiso (~0.3) of the atoms. Further trials during SQUEEZE on structures with/without assigned TBA indicate that applying Platon SQUEEZE[11,12] to all the TBA ions floating in the pore is a more appropriate treatment: For the structure with assigned TBA, R value [$I >= 2\sigma(I)$] before and after SQUEEZE is 11.65% and 8.85%, respectively. In comparison, R value of for the structure without assigned TBA is 14.12% and 7.37% respectively. The fact that 8.85% (assigning TBA) is

higher than 7.37 (not assigning TBA) indicates that the assigned TBA is more disordered than how it is modelled and refined with large-ellipsoid atoms.

Before SQUEEZE was applied, all non-hydrogen atoms were refined anisotropically, and hydrogen atoms were placed in calculated positions. The void volume was estimated to be 13648 Å3 with 4083 electrons removed during SQUEEZE. In the end, Reflections that are affected by the beamstop or having (Iobs-Icalc)/σ > 7 were omitted. The weighting scheme was refined to convergence and the a, b parameters are 0.1482 and 85.9542, respectively.

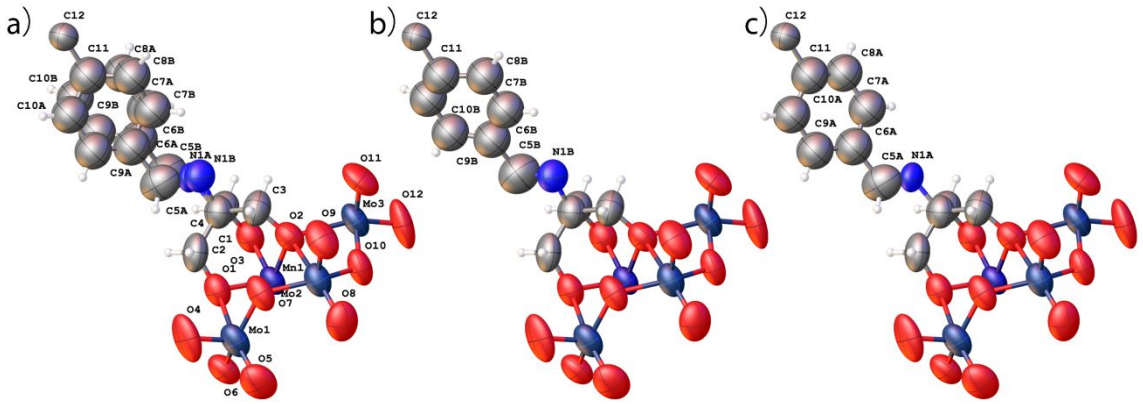

Figure S1. a) Asymmetric unit in the single crystal structure of MOF-688. b) and c) close look at the disordered position A and B of benzene rings on TFPM. Thermal ellipsoids are drawn with 50% probability.

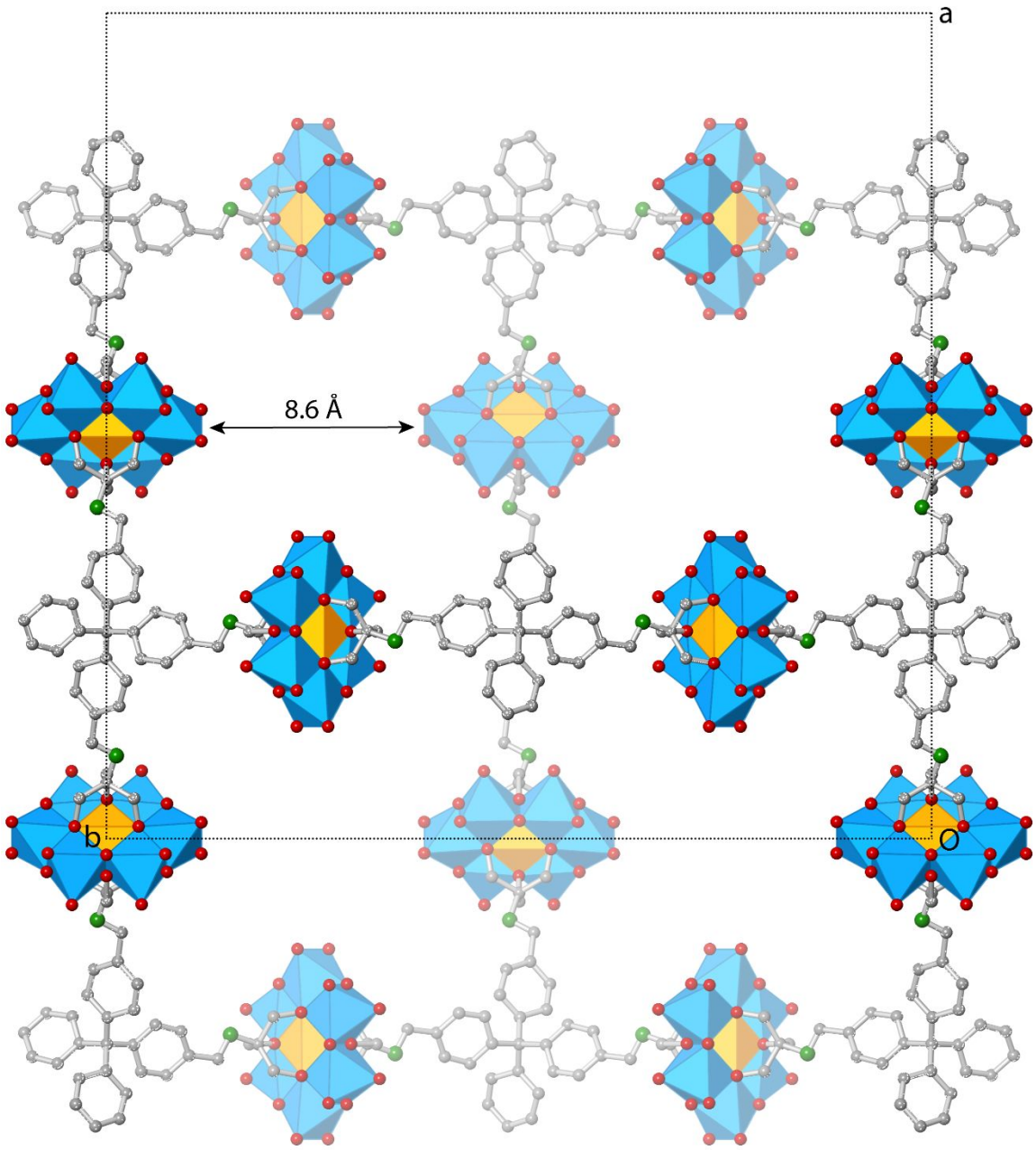

Figure S2. Channel viewed along the crystallographic *c* axis. Mo, blue polyhedra; Mn, orange polyhedra; O, red sphere; N, green sphere; C, gray sphere. Hydrogen atoms and TBA ions are omitted for clarity.

Table S1. Crystal data, data collection, and structure refinement parameters for MOF-688.

Empirical formula	$C_{11.25}H_{10.66}Mn_{0.5}Mo_3NO_{12}$
Formula weight	667.16
Temperature/K	100.0
Crystal system	tetragonal
Space group	$I4_1/a$
a/Å	38.1427(19)
b/Å	38.1427(19)
c/Å	13.6269(7)
α/°	90
β/°	90
γ/°	90
Volume/Å^3	19825(2)
Z	16
ρ_{calc} (g/cm^3)	0.894
μ/mm^{-1}	0.895
F(000)	5115.0
Crystal size/mm^3	0.2 × 0.03 × 0.03
Radiation	Synchrotron (λ = 0.7288)
2Θ range for data collection/°	3.096 to 45.104
Index ranges	$-40 \leq h \leq 40$, $-40 \leq k \leq 40$, $-14 \leq l \leq 14$
Reflections collected	160428
Independent reflections	6041 [R_{int} = 0.0725, R_{sigma} = 0.0326]
Data/restraints/parameters	6041/200/255
Goodness-of-fit on F^2	1.059
Final R indexes [I>=2σ (I)]	R_1 = 0.0737, wR_2 = 0.2282
Final R indexes [all data]	R_1 = 0.0790, wR_2 = 0.2369
Largest diff. peak/hole / e Å^{-3}	0.57/-0.91

Section S4 FT-IR Analysis

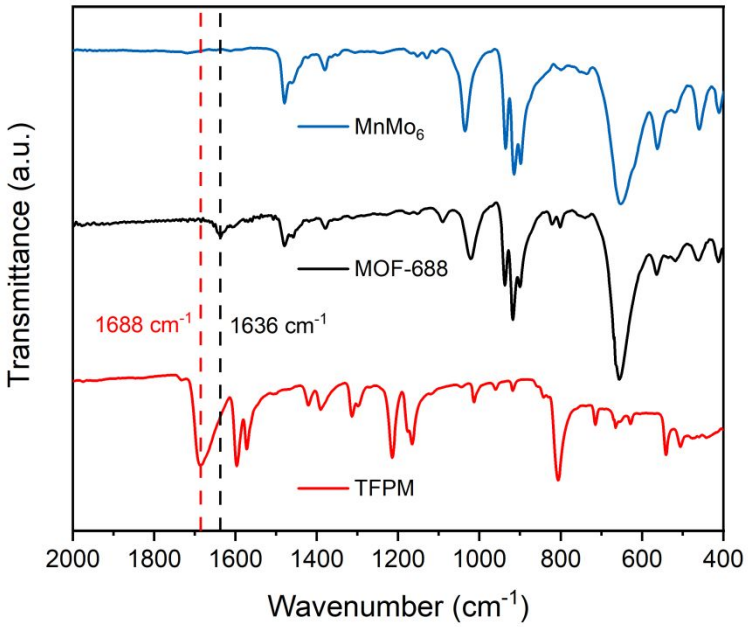

Figure S3. FT-IR spectra of $MnMo_6$, MOF-688, and TFPM.

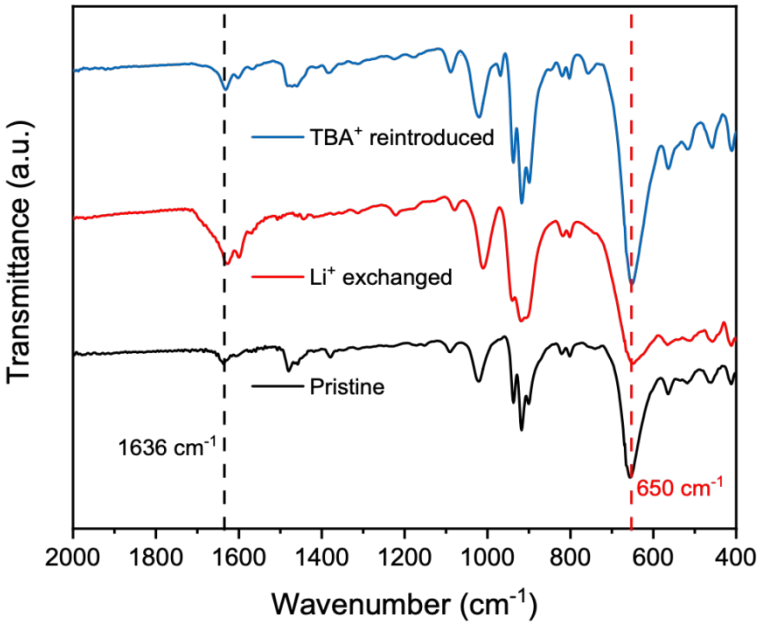

Figure S4. FT-IR spectra of MOF-688 before and after ion exchange. The position of the imine stretch is highlighted.

Section S5 Powder X-ray diffraction of MOF-688

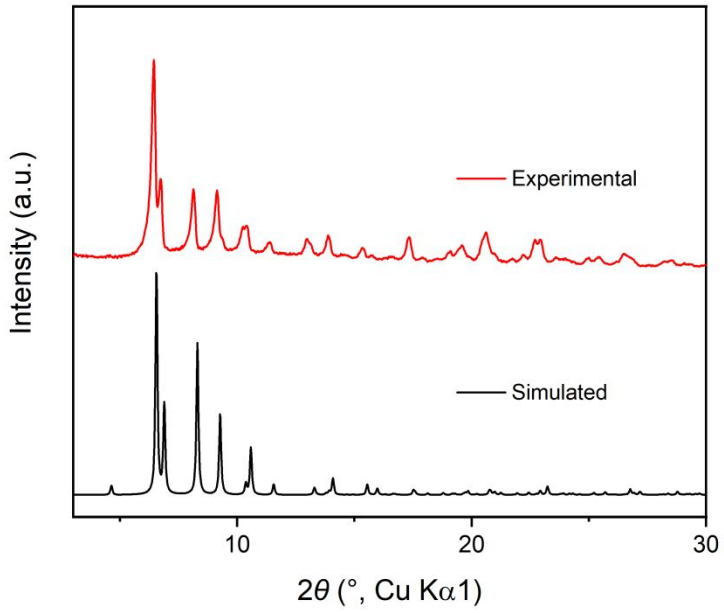

Figure S5. Simulated and experimental PXRD patterns of MOF-688.

×

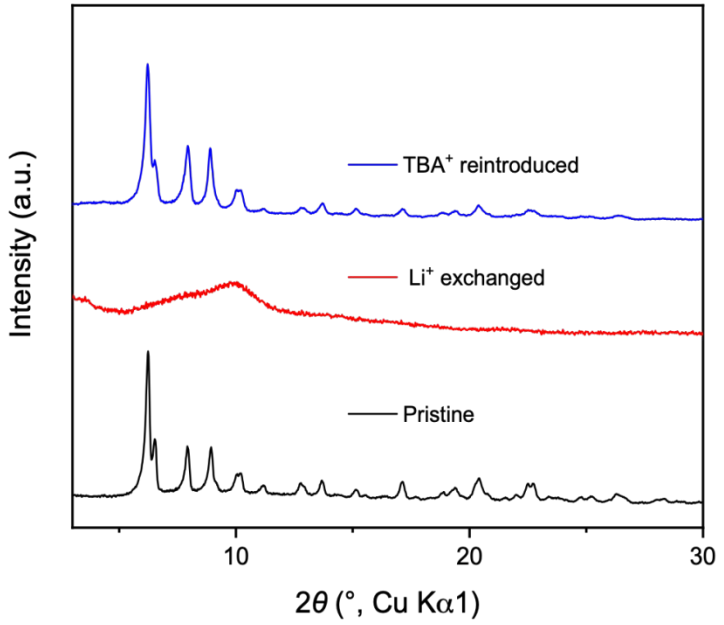

Figure S6. PXRD patterns of MOF-688 before and after ion exchange.

Section S6 Scanning Electron Microscopy of MOF-688

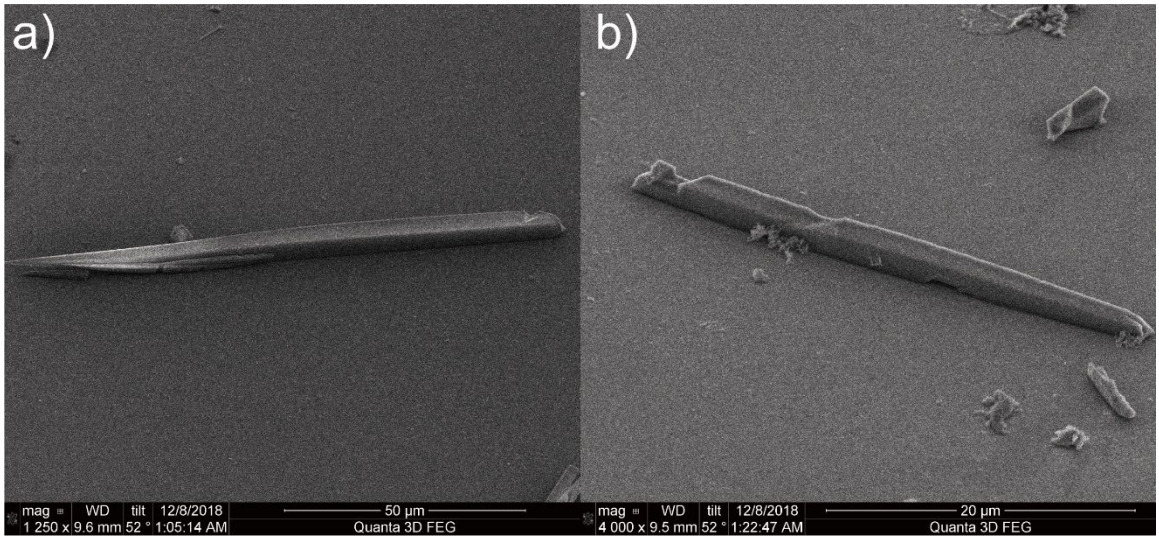

Figure S7. SEM images of MOF-688 (a) before and (b) after Li^+ exchange.

Section S7 Digestion ^{1}H NMR

MOF-688 was digested in a mixture of 10 mg CsF, 50 mL 35 % DCl in D_2O and 550 mL of deuterated dimethylsulfoxide (DMSO-*d*6) for ^{1}H-NMR analysis. The proton signal from the TFPM and TBA^+ cation showed a 1:6 ratio, suggesting a 1:2 ratio between TFPM and $MnMo_6$. The proton signal at 3.43 ppm corresponds to tris(hydroxymethyl)aminomethane, which partially dissociated from $MnMo_6$ during the digestion.[1] The Li^+ exchange process was monitored by digestion ^{1}H NMR, where peaks assigned to TBA^+ disappeared upon cation exchange.

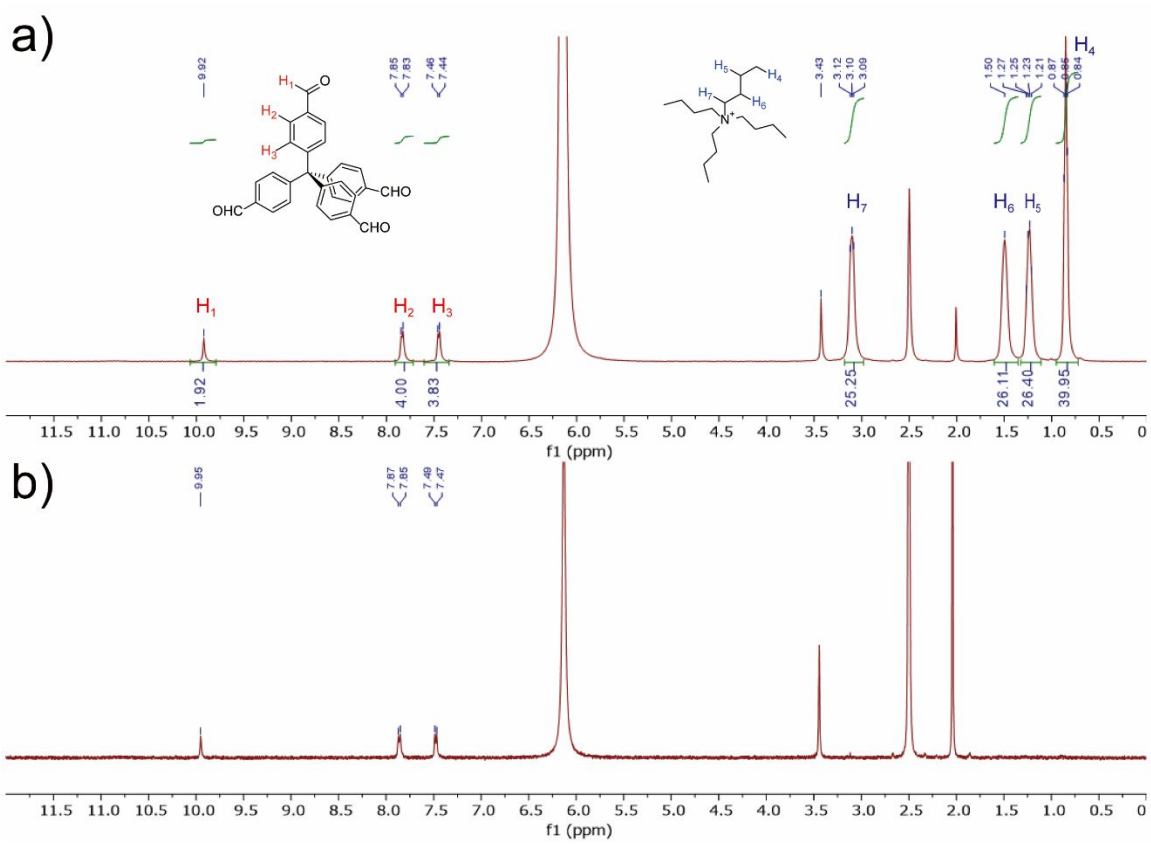

Figure S8. ^{1}H NMR spectra of digested MOF-688 in DMSO-*d*6 (a) before and (b) after Li^+ exchange.

Section S8 Thermogravimetric Analysis

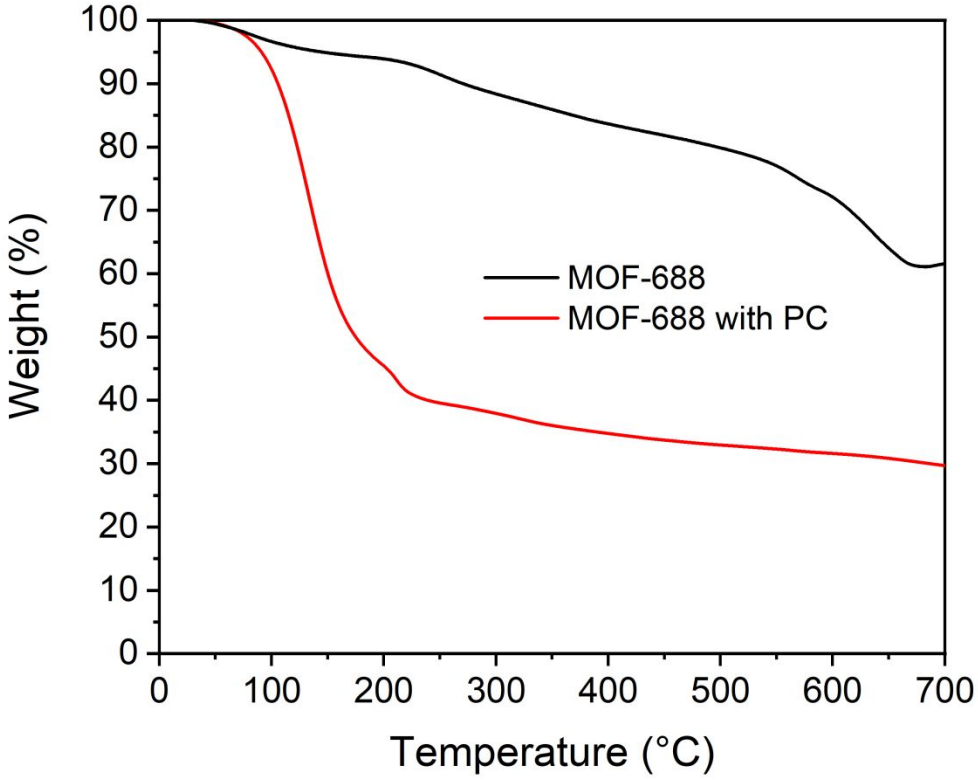

Figure S9. TGA trace of Li^+ exchanged MOF-688 before and after propylene carbonate (PC) solvation measured under continuous flow of nitrogen. The amount of propylene carbonate in MOF-688 was determined by weight loss of solvated MOF-688 at 200 °C.

Section S9 Electrochemical Impedance Spectroscopy

The pellet was prepared in a split-able test cell (MTI Corporation) by hand pressing MOF-688 into a PTFE cylindrical die with 10 mm diameter in an Ar filled glovebox. The pellet was then sandwiched between two stainless steel blocking electrodes. The thickness of the pellet is 1.0 mm determined by the thickness of the mode.

The alternating current (AC) impedance analysis was performed using a two-probe method with a Bio-logic VMP3 potentiostat/galvanostat with an input voltage amplitude of 10 mV between 1 MHz and 1 Hz. Data was recorded from 60 °C to -40 °C with a 10 °C interval. The temperature of the cell was maintained at the target temperature for two hours in an Espec SH-242 chamber before each measurement. The resistance was obtained from the Nyquist plot[3]. The ionic conductivity was calculated using equation (1),

$$\sigma = \frac{l}{RA} \tag{1}$$

where σ is ionic conductivity, l is the pellet thickness, A is the pellet area, and R is the resistance obtained from the measurement.

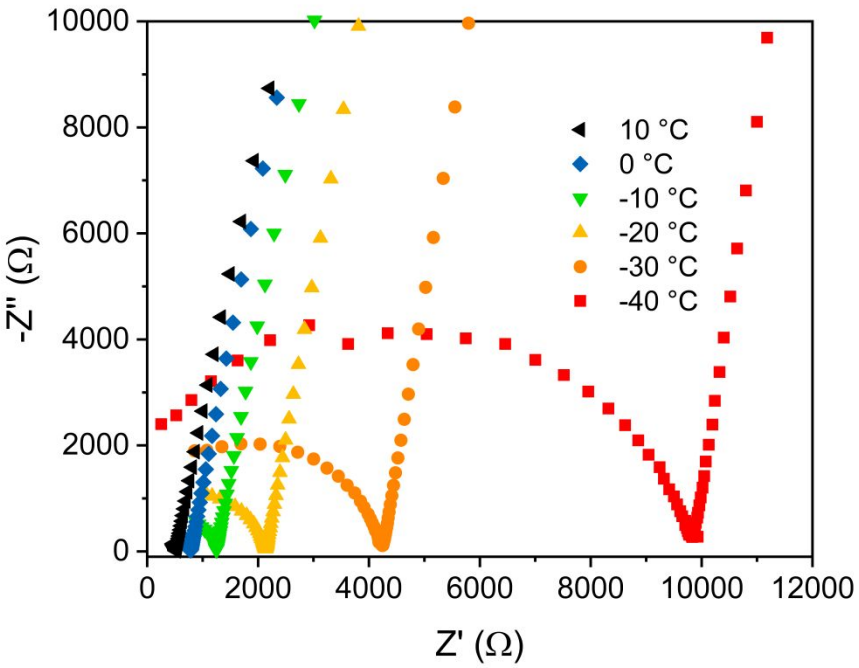

Figure S10. Nyquist plots of MOF-688 from -40 °C to 10 °C.

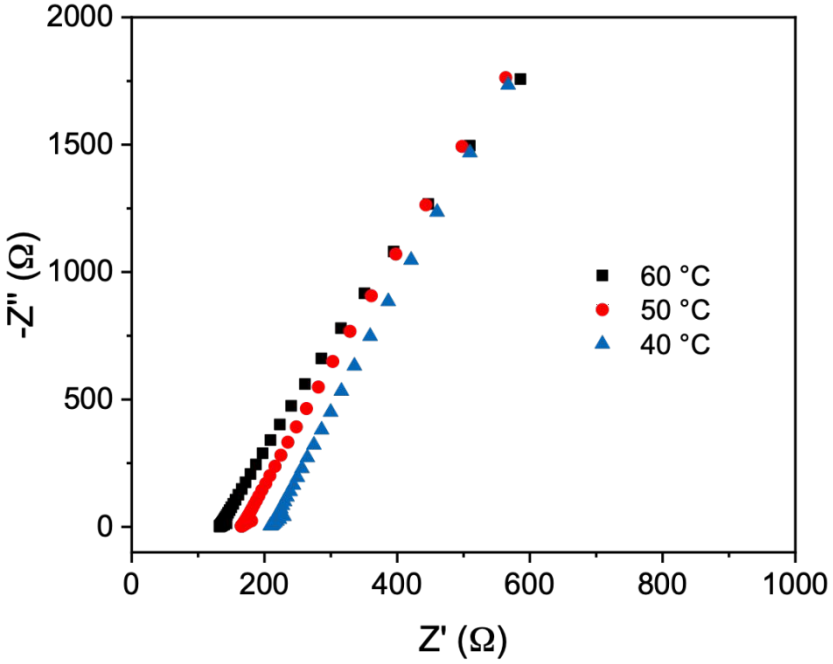

Figure S11. Nyquist plots of MOF-688 from 40 °C to 60 °C.

Section 10 Measurements of Li^+ Transference Number

MOF-688 was suspended in acetone and mixed with a *N*-methyl-2-pyrrolidone (NMP) solution of polyvinylidene fluoride (PVDF) in a 3 to 1 weight ratio. The acetone was subsequently removed under vacuum. The obtained slurry was casted onto a porous cellulose support (Kimwipe) and dried at 85 °C for 24 h. Discs of Φ = 19 mm were punched from the dried film to obtain membrane separators. Li^+ exchange of the MOF-688 membrane was carried out following the same procedure as described for MOF-688 powders. The Li^+ exchanged membrane was immersed in anhydrous propylene carbonate (5 mL × 3) over three days before characterization. The film was assembled into the cell between two lithium chips (MTI Corporation) of Φ = 16 mm in an Ar filled glovebox.

The direct current (DC) polarization measurement was performed on cells with a 10 mV potential and the current response was measured for 30 min at ambient temperature. The EIS was measured with an input voltage amplitude of 10 mV between 1 MHz and 1 Hz before and after the DC polarization.

Li^+ transference number was calculated using the Bruce-Vincent-Evans (BVE) equation (2),[4]

$$t_{Li^+} = \frac{I_s(\Delta V - I_0 R_0)}{I_0(\Delta V - I_s R_s)} \tag{2}$$

where t_{Li+} is the Li^+ transference number, ΔV is the applied potential, I_0 and I_s are the initial and steady-state current, and R_0 and R_s are the initial and steady-state interfacial resistance. R_0 and R_s are determined by fitting the Nyquist plot using EC-Lab software according to previous reports.[5]

It must be pointed out that when the interfacial resistance is significantly higher than the bulk resistance, most of the voltage is applied onto the interface between electrolyte and lithium, instead of the electrolyte itself. In this scenario, both ΔV-I_0R_0 and ΔV-I_sR_s (which reflect the voltage applied onto the bulk electrolyte) are close to zero. As R_0 and R_s are obtained by fitting the Nyquist plot to the equivalent circuit, errors are usually introduced.[3] This error can be enlarged nonlinearly when $\Delta V \approx IR$, and as a result, calculating Li^+ transference number through equation (2) can lead to unreliable conclusions.

Section 11 Galvanostatic Cycling Measurements on Coin Cell Battery

$LiFePO_4$ cathode slurry was prepared by dispersing 50 mg of $LiFePO_4$, 30 mg of MOF-688, 10 mg of Super C45 and 10 mg of PVDF in 1 mL NMP. 20 μL of the cathode slurry was cast onto the MOF-688 film within a region of 1 cm^2 and dried at 85 °C for 24 h. The black colored cathode material was only observed on one side of the MOF-688 film. The Li^+ and solvent exchange of the film was carried out according to the procedure of Section 10. The film was then assembled into a CR2032 coin cell with a lithium chip as the anode in an Ar filled glovebox. The coin cell was allowed to rest for 24 h before measurement.

Galvanostatic cycling measurements were carried out by cycling the battery between 3 V and 3.8 V with a current density of 30 mA g^{-1} at ambient temperature and the voltage response was recorded every 10 s.

References

(1) Marcoux, P. R.; Hasenknopf, B.; Vaissermann, J.; Gouzerh, P. Developing Remote Metal Binding Sites in Heteropolymolybdates. *Eur. J. Inorg. Chem.* **2003**, *2003*, 2406–2412.

(2) Li, Z.; Li, H.; Guan, X.; Tang, J.; Yusran, Y.; Li, Z.; Xue, M.; Fang, Q.; Yan, Y.; Valtchev, V.; Qiu, S. Three-Dimensional Ionic Covalent Organic Frameworks for Rapid, Reversible, and Selective Ion Exchange. *J. Am. Chem. Soc.* **2017**, *139*, 17771–17774.

(3) Qian, X.; Gu, N.; Cheng, Z.; Yang, X.; Wang, E.; Dong, S. Methods to Study the Ionic Conductivity of Polymeric Electrolytes Using A.c. Impedance Spectroscopy. *J. Solid State Electrochem.* **2001**, *6*, 8–15.

(4) Evans, J.; Vincent, C. A.; Bruce, P. G. Electrochemical Measurement of Transference Numbers in Polymer Electrolytes. *Polymer* **1987**, *28*, 2324–2328.

(5) Park, S. S.; Tulchinsky, Y.; Dincă, M. Single-Ion Li^+, Na^+, and Mg^{2+} Solid Electrolytes Supported by a Mesoporous Anionic Cu–Azolate Metal–Organic Framework. *J. Am. Chem. Soc.* **2017**, *139*, 13260–13263.

(6) *APEX3*, version 8.38; Bruker-AXS: Madison, WI 2018.

(7) *SADABS*, Version 2014/4; Bruker-AXS: Madison, WI 2014.

(8) Sheldrick, G. M. A short history of SHELX. *Acta Cryst. A*. **2008**, *64*, 112–122.

(9) Sheldrick, G. M. Crystal structure refinement with SHELXL. *Acta Cryst. C.* **2015**, *71*, 3–8.

(10) Dolomanov, O. V.; Bourhis, L. J.; Gildea, R. J.; Howard, J. A. K.; Puschmann, H.; OLEX2: a complete structure solution, refinement and analysis program. *J. Appl. Crystallogr.* **2009**, *42*, 339–341.

(11) Spek, A. L.; Structure validation in chemical crystallography. *Acta Crystallogr., Sect. D: Struct. Biol.* **2009**. D65, 148–155.

(12) Spek, A. L.; PLATON SQUEEZE: a tool for the calculation of the disordered solvent contribution to the calculated structure factors. *Acta Crystallogr., Sect. C: Struct. Chem.* **2015**, C71, 9–18.